INTERNAL ACOUSTICS MEASUREMENTS OF A FULL SCALE ADVANCED DUCTED PROPULSOR DEMONSTRATOR

O.L. Santa Maria*
NASA Langley Research Center
Hampton, Virginia

P.T. Soderman†, W.C. Horne
NASA Ames Research Center
Moffett Field, California

M.G. Jones
Lockheed Engineering & Sciences Co.
Hampton, Virginia

L.A. Bock
United Technologies, Pratt & Whitney Aircraft
East Hartford, Connecticut

Abstract

Acoustics measurements of a Pratt & Whitney full-scale ADP (Advanced Ducted Propulsor), an ultra-high by-pass ratio engine, were conducted in the NASA Ames 40- by 80-Foot Wind Tunnel. This paper presents data from measurements taken from sensors on a fan exit guide vane in the ADP. Data from two sensors, one at mid-span and the other at the tip of the fan exit guide vane, are presented. At the blade passage frequency (BPF), the levels observed at the various engine and wind speeds were higher at the mid-span sensor than the tip sensor. The coherence between these internal sensors and external microphones were calculated and plotted as a function of angle (angles ranged from 5° to 160°) relative to the ADP longitudinal axis. At the highest engine and wind speeds, the coherence between the tip sensor and the external microphones was observed to decrease at higher multiples of the BPF. These results suggest that the rotor-stator interaction tones are stronger in the mid-span region than at the tip.

Introduction

The requirement for increased fuel efficiency and reduced noise in aircraft operations has lead to the investigation of an ultra-high by-pass ratio engine for commercial aircraft of the 21st century. One engine configuration under consideration is an ADP (Advanced Ducted Propulsor), characterized by ultra-high by-pass ratio, very low fan pressure ratio, large diameter, and very low fan rotational speeds. The low fan speeds are achieved through the use of a gear box, allowing the engine's low rotor and fan to run at different and optimum speeds.

ADP's will have by-pass ratios of 10 to 20 and, depending on the airframe application, fan diameters as large as 160 inches. Noise concerns resulting from such large fans and annular ducts are offset by the characteristically low fan speeds. However, fan noise is still expected to be the major noise contributor to the total engine noise. Therefore, it is important to

* Member AIAA
† Associate Fellow AIAA

investigate the fan noise characteristics of this type of engine.

A 17-in. diameter ADP model was previously tested in various facilities. Acoustics measurements were obtained in the United Technologies Research Center's Acoustic Research Tunnel (ART), and the NASA Lewis Low-Speed Anechoic Wind Tunnel. Results from the NASA Lewis tests can be found in ref. 1.

This paper presents results of internal acoustics measurements made during an acoustic test of the Pratt & Whitney full scale ADP Demonstrator conducted in the NASA Ames 40- by 80-ft wind tunnel in August 1993. The sound pressure levels (SPL) on a stator at the Blade Passage Frequency (BPF) will be shown for various engine and wind speeds, followed by some coherence data between the external microphones and internal acoustics sensors.

Description of Experiment

Wind Tunnel

The Ames 40-by 80-Foot Wind Tunnel (40 x 80) is a closed-circuit wind tunnel with a closed test section. Six 40-ft diameter fans are located in the drive section in two horizontal rows of three fans each. The variable-speed, variable-pitch fans can be operated from 0 to 180 rpm with blade-pitch angles from -18° to 52° relative to the fan disc. The maximum mass flow results in an airspeed of approximately 300 knots in the test section. Airspeeds of 20, 50, 100, and 140 knots were selected to be tested with each engine speed for this experiment.

The 80-ft long test section is connected to the settling chamber by an 8 to 1 contraction. Not counting the acoustic lining insert, the test section has flat, 40-ft wide, floor and ceiling sections, and semicircular walls that create a test section 39 ft high and 79 ft wide (40- by 80-ft). A 34.5-ft diameter turntable covering a six-component balance system is located in the center of the test-section floor.

The test-section walls, exclusive of the floor, are lined with a 0.5 ft deep sound absorbent lining composed of fiberglass bats wrapped in cloth and covered with a 40% open area perforated steel plate. The floor lining is similar, but contains a 0.12-ft thick steel grating for support of personnel and equipment, that leaves a 0.37-ft thick fiberglass layer below the grating. The sound absorption of the tunnel lining shown is marginal at the frequencies of interest, with a sound absorption coefficient near 0.65 at 350 Hz (ref. 2).

ADP Demonstrator

The model was a Pratt & Whitney ADP demonstrator engine with a 19.1-ft long nacelle, constructed from a modified PW2037 core. The modifications included the addition of a 40,000 HP gear box which drives a 9.8-ft diameter fan. Figure 1 is a schematic cross-sectional side view of the ADP. The fan was comprised of 18 blades. There were 45 fan exit guide vanes or stators in the stator row aft of the fan and 10 circumferentially distributed struts aft of the stator row. The pitch of the fan blades was variable so that the fan could be feathered and driven to reverse pitch, which would eliminate the need for a conventional fan duct thrust reverser. The by-pass ratio (fan air/jet air) was about 14. The high by-pass ratio and reduced fan rotational speed (as compared to existing engines) was expected to result in higher fuel efficiency and reduced noise.

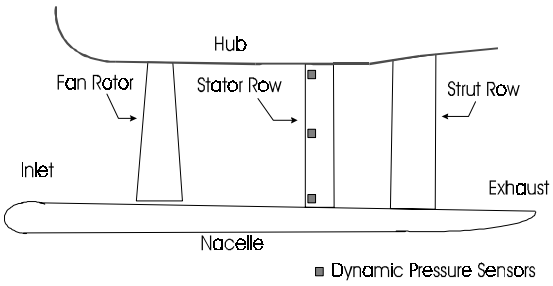

Figure 1. Schematic of ADP axial cross-section.

For this test, the engine was operated at 0° angle of attack and 0° yaw angle. Model thrust and drag were measured with the wind tunnel balance system, which has a 24,000 lb limit that restricted the fan operating cycle to 45% of full thrust. Five engine speeds, with the following fan rotor speeds were measured: 0, 901, 1110, 1210, and 1310 rpm. These engine speeds were chosen to match those of a previous test conducted with the full scale ADP on Pratt & Whitney's outdoor test stand in Florida. Fan blades were set at a stagger angle corresponding to the approach condition throughout the acoustics test.

The ADP was mounted near the test section center and was hung from a faired structural beam system which spanned two large struts and was connected to a

smaller aft strut. The aft strut was offset from the engine exhaust to minimize flow impingement. Figure 2 shows the layout of the test section as viewed from above the model.

Data Acquisition

The internal acoustics measurements were made with Endevco dynamic pressure sensors installed on a stator at the 168° position (0° corresponded to top center). These sensors had a pressure range of 0 to 15 psia and were surface mounted on the leading edge of the suction side of the fan exit guide vane. The locations were 0.10 of the chord length behind the leading edge, at 0.10 (hub), 0.50 (mid-span), and 0.90 (tip) of the span, as shown in Figure 3. This arrangement followed that of a ONERA test described in ref. 3. Unfortunately, the sensor closest to the engine hub was not functioning properly and no reliable data were acquired at this position.

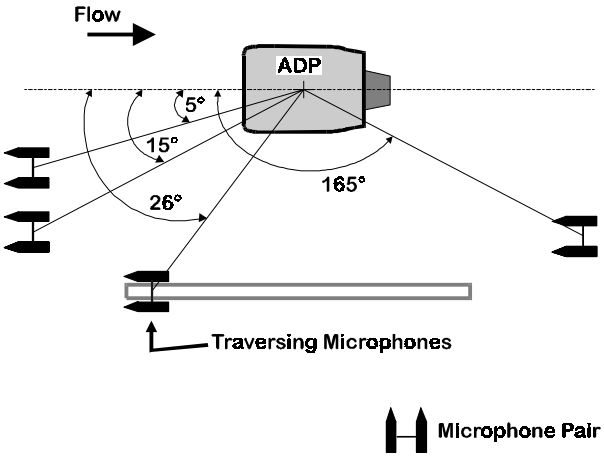

Figure 2. 40- by 80-ft wind tunnel test section layout (not to scale, support structure not shown).

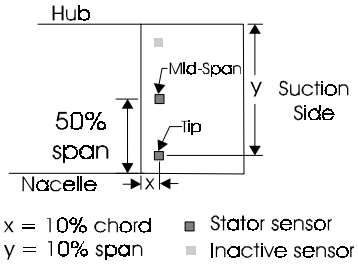

Figure 3. Stator sensor positions (not to scale).

External acoustics data were acquired with a traversing microphone system (ref. 4), as seen in Figure 2. These enabled sideline noise measurements 18 ft from the engine centerline at the engine height. The traverse carried a microphone pair which was stopped at selected angles from 25° to 150°, relative to the flight direction, as measured from a reference point near the engine center. Data were averaged for approximately 30 seconds at each angle. Fixed microphones were also located at angles of 6°, 15°, and 160°. Results of the external microphone measurements will be published in another report.

Eleven channels were used to record the acoustic data on a 14-track MARS 2000 recorder, using one-inch FM analog tape. Data from the sensors on the stator, two in-duct sensors and up to 6 of the microphones were recorded. The other three tracks were used to record the one-per-revolution (1/rev) signal, the time code, and voice.

The tape speed of 30 inches per second (ips) used during the test determined the frequency range of 0 to 20 kHz. Prior to input to the tape recorder, each of the data signals was passed through a Precision Filters filter. This instrument was used to band-pass each of the channels over a selected frequency range. The microphone signals were band-passed from 1 Hz to 20 kHz, the internal dynamic pressure sensors were band-passed from 100 Hz to 20 kHz, and 1/rev signal was band-passed from 10 Hz to 20 kHz.

Calibration

The stator sensors were calibrated using a NASA-Langley calibrator, which consisted of an acoustic driver installed in a metal box. A signal generator was used to supply a 1 kHz sinusoidal signal to the acoustic driver. The pure tone from the acoustic driver was output via copper tubing inside, and a flexible hose outside, the box. The copper tubing and flexible hose were selected to ensure virtually no sound leakage through the walls.

The acoustic driver output was calibrated using a pre-calibrated Endevco transducer installed in another metal box. The flexible hose was placed tightly over the transducer, and the voltage response of the transducer was read with an RMS voltmeter. The amplitude of the sinusoidal input to the acoustic driver was varied until the voltage response matched that expected for a 131 dB (0.1 psi dynamic pressure) pure tone at 1 kHz.

The external microphones were calibrated using a Bruel & Kjaer pistonphone calibrator. The level used to calibrate the microphones was 124 dB at 250 Hz.

Data Reduction

The FM tape data were digitized using Pacific Instruments Model 9830 Analog-to-Digital devices. These 12-bit instruments were used to acquire 524,288 data points per channel per run. The acceptable voltage range is -10 V to +10 V; thus, the ΔV is 4.88 mV. The sample rate for this digitization was chosen to be 62.5 kHz, which resulted in a Δt of 16 μsec. This sample rate was chosen such that aliasing effects could be properly eliminated for analysis frequencies throughout the 20 kHz bandwidth.

The data set for a selected channel was divided into blocks of 4096 data points, with each block beginning at the point where a blip was observed in the 1/rev data. Since the blips did not necessarily occur at every 4096th point, data which fell between the end of one analysis block and prior to the next blip were not used in the analysis. This procedure allowed the data to be analyzed using a signal enhancement technique which causes non-coherent signals to be "averaged out." This was important in extracting pure tone signals from a broadband noise background.

The blocks of data were used in two ways. One was a Fast Fourier Transform (FFT) to obtain narrowband spectra, such as those shown in Figure 4. The other was calculation of the coherence between the microphone signals and the stator sensor signals. The coherence, $\gamma_{xy}^2(f)$, is given in ref. 5 as

$$\gamma_{xy}^2(f) = \frac{\left|G_{xy}(f)\right|^2}{G_{xx}(f)G_{yy}(f)}$$

$$0 \le \gamma_{xy}^2(f) \le 1$$

where G_{xy} is the cross-spectral density of the two signals, and G_{xx} and G_{yy} are the autospectral densities of the two signals x and y, respectively. Data points in both the spectra and coherence are separated by 15 Hz.

Results

Background Levels

Figure 4 shows the spectra of the mid-span stator sensor, with the ADP on and off (rotor locked), for the highest wind and engine (for ADP on) speeds. The levels at the BPF and its multiples were compared with the ADP on and off, for wind tunnel speeds of 20, 50, 100, and 140 knots. With the ADP on, levels were typically found to be at least 10 dB or higher than those with the ADP off. Flow noise was therefore not considered a significant contributor to the BPF levels for the stator sensors.

Effect of Stator Position

The sound pressure levels at the BPF, 2xBPF and 3xBPF for both stator sensors were compared to assess the effect of stator position on the rotor-stator interaction tones. The comparisons for the BPF levels are presented in Figure 5. Consistent among the 3 frequencies was the trend followed by the levels at the stator tip as the wind speed increased. At 20 knots, levels at the tip were higher than at mid-span by 5 to 10 dB. At 50 knots, levels at the tip dropped slightly and began to cross over to below the levels at mid-span. At 100 and 140 knots, the levels at mid-span were higher than at the tip for the BPF, 2xBPF, and 3xBPF tones.

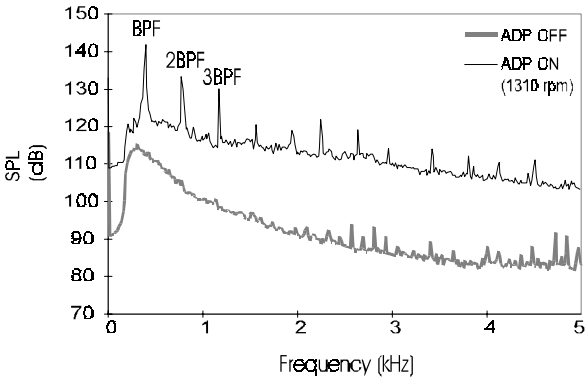

Figure 4. Spectra for mid-span stator sensor. Wind speed = 140 knots.

Levels for the BPF tones at mid-span did not vary as much for the entire wind speed range. In most cases, they were within 5 dB for any given fan speed as the speed increased from 20 to 140 knots.

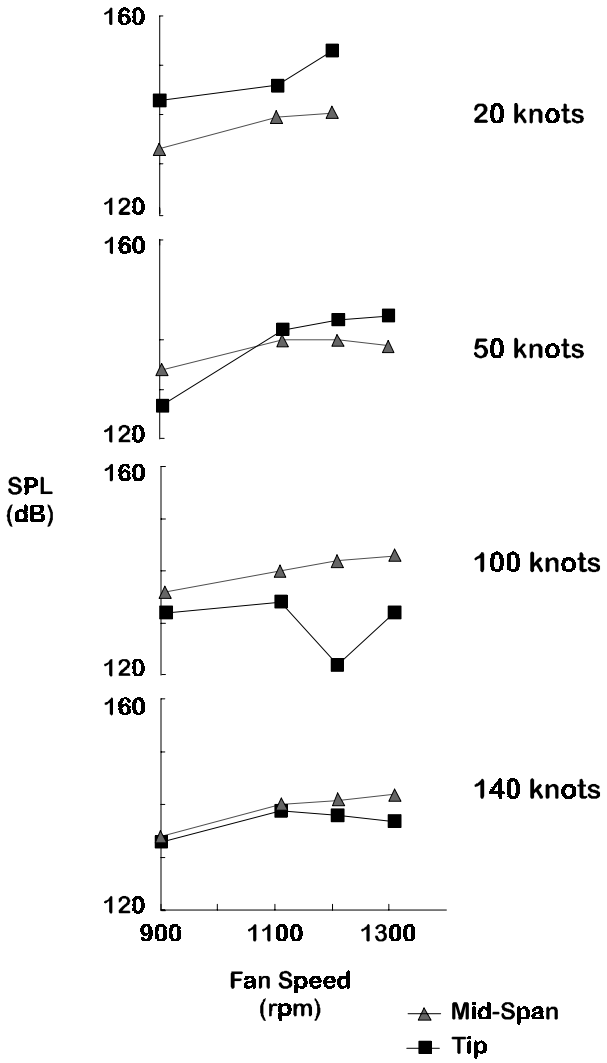

Figure 5. Levels at the blade passage frequency (BPF) at the stator sensors for various wind speeds.

Coherence

Figure 6 shows the directivity of the coherence between the stator sensors and the external microphones for the the BPF, 2xBPF, and 3xBPF tones. The wind speed was 144 knots and the fan rotor speed was 1310 rpm.

The angles shown are referenced to the fan rotor plane (0° in the upstream direction). Below 20°, the data points are from the fixed microphones, as is the final point at 161°. The points at the angles between these fixed positions are plotted separately for the two traversing microphones. Figure 6 shows the directivity of the coherence between the microphones and the stator sensors for the BPF, 2xBPF, and 3xBPF.

The duct modes that cut on are expected to produce peaks in the directivity pattern in the far field. Since the coherence is a comparison of the spectra of two signals, the lobes generated by these cut on modes could appear in the coherence directivity. There is a generally U-shaped pattern in the coherence plots at 2xBPF and 3xBPF, with the coherence higher in the forward and aft angles. The coherence directivity at the BPF does not show this pattern. This is to be expected as no acoustic duct modes should cut on at the BPF, given the number of fan blades and fan exit guide vanes (ref. 6). The coherence at BPF is high, however, most likely due to rotor-alone noise.

The peak angles of the modes that were expected to cut on were calculated using a formulation by Rice (ref. 7) that utilizes the mode cutoff ratio. Only a few of the peak angles from higher order modes lined up with the “peaks” on the above plots, so they could not be attributed to any one mode. Also, due to the rather large intervals between data points, it is unclear if any actual peaks were measured.

An observation to be noted is a comparison between the coherence at the tip and at the mid-span stator sensors. At the BPF, the difference between the coherence plots of the two sensors is small. At 2xBPF and 3xBPF, however, the difference in coherence is as high as 0.24, as shown in Figure 6c. This indicates that the energy in the mid-span region contributes more to the far field radiation at these multiples of the BPF than the energy in the tip region. This is counter-intuitive to the idea of rotor-stator-interaction-generated tones, which are thought to be stronger in the tip region. There may be a sufficient difference in the rotor wake structure between the tip and mid-span regions to cause a lower coherence at the tip.

Summary

Acoustics data from internal measurements of a Pratt & Whitney full-scale ADP (Advanced Ducted Propulsor), an ultra-high by-pass ratio engine, were presented. Data were obtained during a test conducted in the NASA Ames 40- by 80-Foot Wind Tunnel. Data from two sensors, one at mid-span and the other at the tip of the fan exit guide vane were presented. Coherence data between these fan exit guide vane sensors and external microphones were also presented.

At the blade passage frequency (BPF), the levels observed at the various engine and wind speeds were higher at the mid-span sensor than the tip. The directivity of the coherence between these internal sensors and external microphones were plotted for fan rotor speed of 1310 rpm and 144 knots wind speed.

The coherence directivity plots showed a U-shaped pattern at 2xBPF and 3xBPF, but not at the BPF. There was high coherence at the BPF, attributable to rotor-alone noise, as the rotor-stator interaction modes do not cut on at this frequency.

The coherence of the BPF and its multiples, between the tip sensor and microphones, was consistently lower than that of the mid-span sensor, for the highest engine and wind speeds. The difference between the coherence of the tip sensor and microphones and that of the mid-span sensor was observed to decrease at 2xBPF and 3xBPF by as much as 0.24.

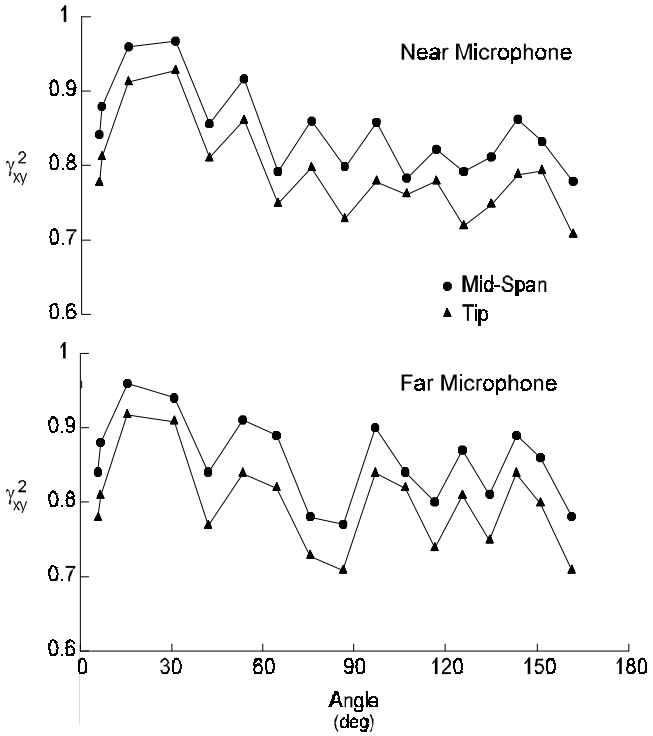

(a) Blade Passage Frequency (BPF)

Figure 6. Coherence Directivity. Wind Speed = 144 knots, Fan Rotor Speed = 1310 rpm.

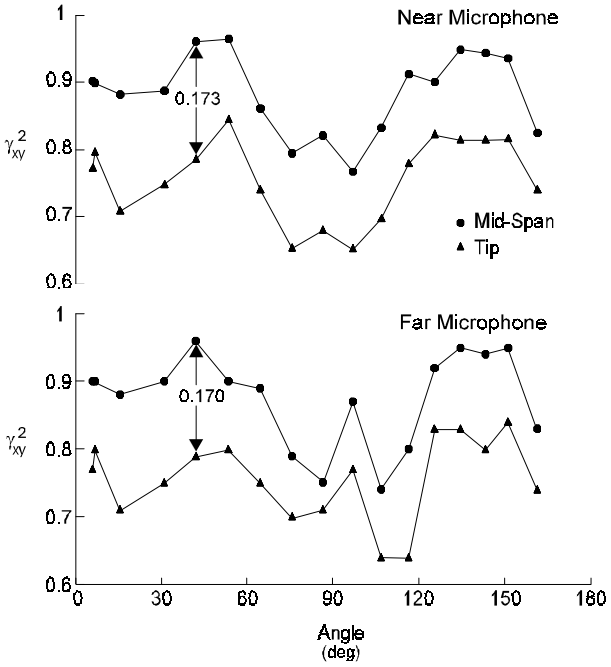

(b) 2 x BPF

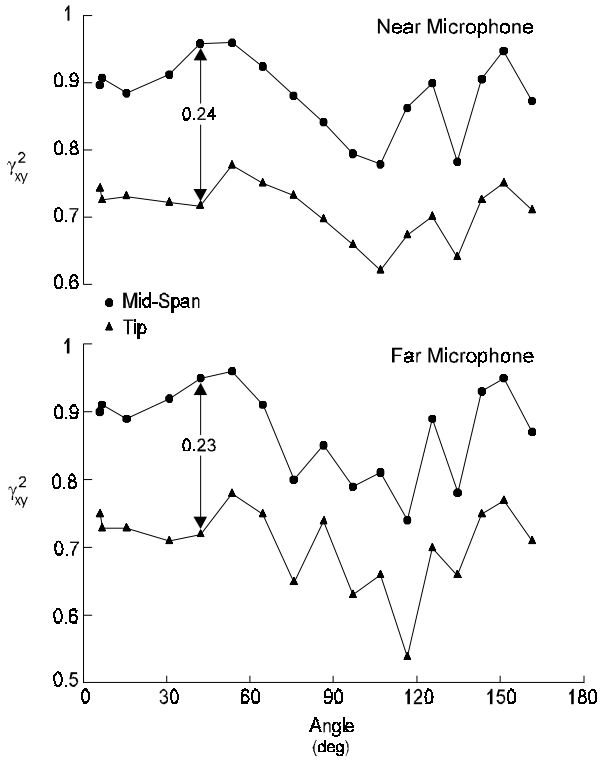

(c) 3 x BPF

Figure 6 (cont.). Coherence Directivity. Wind Speed = 144 knots, Fan Rotor Speed = 1310 rpm.

These observations from data presented imply that the rotor-stator interaction tones are stronger in the mid-span region than at the tip. The cause of this phenomenon is unknown; however, it is postulated that a significant difference in the rotor wake structure impinging on the fan exit guide vanes is a contributor.

References

1. Woodward, Richard P., Bock, Lawrence A., Heidelberg, Laurence J., Hall, David G., "Far-field noise and internal modes from a ducted propeller at simulated aircraft takeoff conditions," NASA-TM-105369, 1992.

2. Soderman, P.T., "Sources and levels of Background Noise in the NASA Ames 40-by 80-Foot Wind Tunnel - A Status Report," NASA-TM-100077, May 1988.

3. Lewy, S. and Canard-Caruana, S., "Experimental Study of Noise Sources and Acoustic Propagation in a Turbofan Model," AIAA Paper 90-3950, October 1990.

4. Jaeger, Stephen M; Allen, Christopher S; and Soderman, Paul T, "Reduction of Background Noise in the NASA Ames 40- by 80-Foot Wind Tunnel," CEAS/AIAA Paper 95-152, AIAA 16th Aeroacoustics Conf, Munich, Germany, June 1995.

5. Bendat, J.S. and Piersol, A.G., *Engineering Application of Correlation and Spectral Analysis,* Second Edition, Wiley & Sons, New York, 1993.

6. Tyler, J.M. and Sofrin, T.G., "Axial Flow Compressor Noise Studies," SAE Aeronautic Meeting, 1961.

7. Rice, E.J. and Heidmann, M.F., "Modal Propagation Angles in a Cylindrical Duct with Flow and their Relation to Sound Radiation," AIAA Paper 79-0183, January 1979.